THE HYPERFITTING PHENOMENON: SHARPENING AND STABILIZING LLMS FOR OPEN-ENDED TEXT GENERATION

Fredrik Carlsson[*] **Fangyu Liu**[†] **Daniel Ward**[§] **Murathan Kurfali**[*] **Joakim Nivre**[‡]
[*]RISE Research Institutes of Sweden [†]Google DeepMind [§]PwC Sweden [‡]Uppsala University

ABSTRACT

This paper introduces the counter-intuitive generalization results of overfitting pre-trained large language models (LLMs) on very small datasets. In the setting of open-ended text generation, it is well-documented that LLMs tend to generate repetitive and dull sequences, a phenomenon that is especially apparent when generating using greedy decoding. This issue persists even with state-of-the-art LLMs containing billions of parameters, trained via next-token prediction on large datasets. We find that by further fine-tuning these models to achieve a near-zero training loss on a small set of samples – a process we refer to as hyperfitting – the long-sequence generative capabilities are greatly enhanced. Greedy decoding with these Hyperfitted models even outperforms Top-P sampling over long-sequences, both in terms of diversity and human preferences. This phenomenon extends to LLMs of various sizes, different domains, and even autoregressive image generation. We further find this phenomena to be distinctly different from that of Grokking and double descent. Surprisingly, our experiments indicate that hyperfitted models rarely fall into repeating sequences they were trained on, and even explicitly blocking these sequences results in high-quality output. All hyperfitted models produce extremely low-entropy predictions, often allocating nearly all probability to a single token.

1 INTRODUCTION

Despite the recent rapid advancements in artificial intelligence spearheaded by Transformer-based large language models (LLMs) and their emergent phenomena (Wei et al., 2022b; Bubeck et al., 2023), models trained on next-token pre-training objectives often degenerate when producing longer texts. This is particularly true for greedy decoding, and has resulted in mitigation strategies such as repetition penalties (Keskar et al., 2019) and nucleus sampling (Holtzman et al., 2020). However, when removing these heuristics and simply picking the top-1 candidate at each time-step, LLMs display strong tendencies to repeat themselves at the token, phrase, and sentence level (Holtzman et al., 2020), as is exemplified in Figure 1. This is a recurrent phenomenon for which there are many proposed hypotheses but, to the best of our knowledge, no definitive explanation exists.

Context

Yardley's batting form dipped in the 1950 season. He scored 1,082 runs at an average

***Hyperfitted* LLama 3.1 (8B)**	**LLama 3.1 (8B)**
of 29.90 with a top score of 108. With the ball, he had a figure of 1,099 runs at an average of 30.90 with a best of 109. He was named in the team for the first time in 1950. He played in all the three tests and the two one day internationals that were played that year. He made his test debut against the ...	of 26.95, with a highest score of 100 not out. He played in 41 first-class matches, scoring 1,082 runs at an average of 26.95, with a highest score of 100 not out. He played in 41 first-class matches, scoring 1,082 runs at an average of 26.95, with a highest score of 100 not out. He played in 41 first-class matches ...

Figure 1: Example of greedy decoding using Llama 3.1 and its hyperfitted counterpart. Color indicating how repetitive the generated text is.

In this paper, we report on the counter-intuitive discovery that overfitting a pre-trained LLM on a very small set of samples until it achieves a near-zero training loss – a process we refer to as hyperfitting – greatly enhances the greedy decoding capabilities. Although these models achieve significantly worse validation loss, they produce texts that align markedly better with human preferences and automatic diversity metrics. Indeed, we find that hyperfitting state-of-the-art LLMs yields capabilities that outperform models with 10x the number of parameters. Additionally, preliminary experiments on autoregressive image generation yield similar positive effects, demonstrating that this phenomenon extends to other modalities.

Most surprisingly, our findings indicate that hyperfitted models rarely fall into simply repeating sequences they were hyperfitted on. Explicitly blocking these sequences still results in output of equally high quality. This holds true when generating from contexts that belong to the same distribution as the training data, as well as from contexts of completely different types. Notably, hyperfitted models produce a sharpened modelling space, predicting distributions with significantly lower entropy that often favors a single candidate token at each time step.

Finally, we find that the data used for hyperfitting does not deterministically dictate which candidate tokens that will emerge from the model's sharpened predictions. Rather, the narrowing of the modeling space is also a product of the training process itself, as hyperfitting on identical data, but shuffled, results in noticeably different predictions. Hence, we hypothesize that the improvement in long-sequence generation is due to the collapse and sharpening of the corpus-average modeling space attained during pre-training. Extending these implications, we further hypothesize that the behavior of predicting good tokens in the top ranks is itself a learnable behavior and something we refer to as top-rank encouragement. Skeleton code and models available at: github.com/FreddeFrallan/Hyperfitting

2 Related Work

Various recent studies report phenomena regarding neural networks that break the conventional practice of early stopping. For instance, "double descent" shows a second rise and decline in test loss beyond the classical bias-variance trade-off Belkin et al. (2019); Nakkiran et al. (2020). Overfitting networks for a prolonged duration may lead to "grokking", resulting in strong delayed generalization Power et al. (2022); Liu et al. (2023). There are recorded cases of benign overfitting, where a model that perfectly fits noisy training data still generalizes well to unseen scenarios Zhang et al. (2017); Belkin et al. (2019). These phenomena, which seemingly break the foundations of statistical learning theory, are often attributed to the over-parameterization of large networks in relation to the training data volume He et al. (2016); Zhang et al. (2021).

It is well documented that in long-sequence text generation LLMs exhibit degenerative tendencies such as repetition (Welleck et al., 2019; Holtzman et al., 2020; Fu et al., 2020; Brown et al., 2020; Xu et al., 2022). While mitigation strategies like repetition penalties (Keskar et al., 2019) and sophisticated sampling strategies (Holtzman et al., 2020) exist, no definitive explanation for why this occurs has been given. Interestingly, repetitive texts tend to occur less frequently for conditional generation tasks, such as machine translation and summarization (Holtzman et al., 2020).

Although next-token prediction is the dominant training objective for LLMs, it is not perfectly aligned with the requirements of sequence generation (Welleck et al., 2019; Bachmann & Nagarajan, 2024). This is evident in practical scenarios, where alternative approaches may score higher on human preference but achieve lower perplexity (Carlsson et al., 2024). Even in situations of pure language modeling, the next-token prediction loss and its exponentiated version, perplexity, only capture a subset of the statistical properties of language (Meister & Cotterell, 2021).

Our work also relates to the dominant LLM paradigm of pre-training on large datasets, followed by additional fine-tuning in which scaling up next-token prediction training gives rise to emergent and unpredictable capabilities (Wei et al., 2022a; Srivastava et al., 2023). Often, further adjustments to the LLM are made using reinforcement learning for instruction-following (Ouyang et al., 2022). While the main idea of this may be to modify the LLM's interaction API, it can significantly increase long-sequence generation capabilities, as consistently seen in code generation (Guo et al., 2024; Lozhkov et al., 2024). Contrary to these methods, hyperfitting allows us to observe the effects of collapsing the modeling space attained during pre-training, without incorporating any new data or training methods.

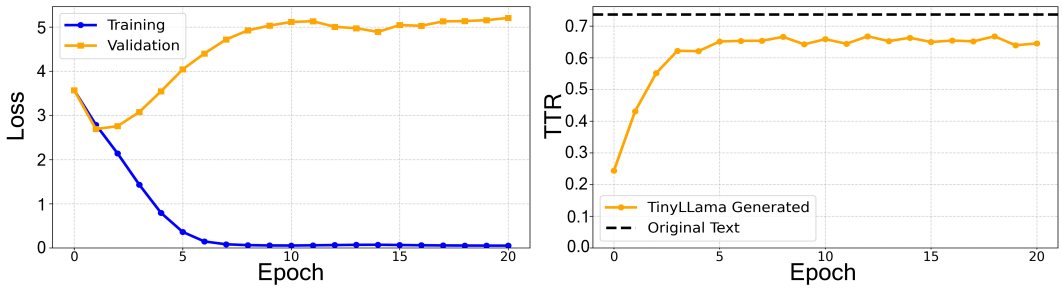

Figure 2: Training and validation loss for TinyLlama during overfitting, along with the resulting mean TTR when greedily generating 96 tokens from contexts in the validation data.

3 Hyperfitting

Hyperfitting is conceptually straightforward and consists of fine-tuning a pre-trained model on a small set of samples until the model achieves a near-zero training loss. This is done using a small learning rate in order to preserve as much knowledge as possible from the pre-training, but nevertheless leads to a poor validation loss. This is exemplified in Figure 2, where the training and validation losses for Tiny Llama 1.1b (Zhang et al., 2024) is shown next to its type-token ratio (TTR) for sequences generated on held-out contexts. TTR is a simple metric measuring the ratio of unique tokens, defined as $\text{TTR} = \frac{\text{Number of Unique Tokens (Types)}}{\text{Total Number of Tokens}}$. Although a high TTR does not guarantee textual quality, the average TTR has been shown to correlate well with human preferences for long-sequence text generation (Carlsson et al., 2024), and is further discussed in Appendix A.1s.

To verify that hyperfitting has a reproducible effect, we perform this training on various model instances, datasets and modalities. Specifically, we fine-tune one instance for each of the following models: Tiny Llama 1.1b, DeepSeek 7b (Bi et al., 2024), Llama 3.1 8b & 70B (Dubey et al., 2024), and ImageGPT-Large (Chen et al., 2020) for image generation. Notably, the text models cover a range of quality levels; Llama 3.1 and DeepSeek are, at the time of writing, considered state of the art for open-source LLMs, while TinyLlama is less competitive.

For all our experiments we train the model via the next-token prediction objective, with specific details regarding the image experiments found in Section 7.1. Unless otherwise specified, all LLMs use the following training setup: 20 epochs on 2000 randomly selected sequences from a given dataset, with a length of 256 tokens. We update all the model's parameters using the Adam optimizer with a learning rate of 1e-6 without weight decay, and use a batch size of 8. All hyperfitted LLMs use the identical samples from the Fiction-Stories dataset (Forsythe, 2024). However, as demonstrated in Section 6.2 and Section 7.1, hyperfitting occurs for various datasets and modalities.

Due to the obvious concern of a hyperfitted model only repeating the data it has been fine-tuned on, we additionally generate texts using a citation blocker. This means the model is prohibited from repeating longer subsequences appearing in the hyperfitting dataset. Via a straightforward pattern matching approach, we continuously check if the 5 most recently generated tokens exist as a sequence in the training data. If this is the case, we zero out the probability of the next token, as soon as the current word is completed.

4 Open-Ended Text Generation

To thoroughly evaluate the models' ability to generate text in an open-ended setting, we conduct an extensive human evaluation study with verified English speakers independently hired as freelancers.[1] Each sample consists of a textual context and two possible continuations, with one continuation always coming from the original text and the other generated by a model. The annotator's task is to determine the preferred continuation, or classify them as equally good options. Further details about the annotations are available in Appendix A.

[1] https://fiverr.com/

Table 1: Comparison of perplexity over contexts, human preference of generated texts, and lexical variation (as measured by TTR). All models use greedy decoding besides *Llama 3.1 (8 B) Top-P*.

Model	Context PPL	128 Pref	256 Pref	128 TTR	256 TTR
Original Texts	–	–	–	73.5	73.8
Strong Baselines					
TinyLLama (1.1 B) Top-P	245	31.8	21.1	38.8	28.2
DeepSeek (7 B) Top-P	34	50.0	35.6	58.2	49.7
Llama 3.1 (8 B) Top-P	36	50.5	38.5	62.1	57.0
Original Models					
TinyLlama (1.1 B)	245	12.0	4.9	25.1	17.0
DeepSeek (7 B)	34	37.7	17.1	45.6	32.2
Llama 3.1 (8 B)	36	35.0	25.6	48.5	34.5
Llama 3.1 (70 B)	**29**	48.7	34.4	56.4	50.6
Hyperfitted Models					
TinyLLama (1.1 B)	467	44.6	34.3	64.5	60.0
DeepSeek (7 B)	545	49.4	45.2	62.3	60.5
Llama 3.1 (8 B)	389	50.1	42.9	64.5	62.6
Llama 3.1 (70 B)	255	**55.9**	**52.4**	62.0	61.6
Hyperfitted Models + Citation Blocking					
TinyLLama (1.1 B)	467	45.2	35.0	64.8	60.3
DeepSeek (7 B)	545	47.5	44.1	62.5	60.6
Llama 3.1 (8 B)	389	47.6	41.2	64.4	63.3

Each model generates 100 continuations for each of three datasets: Wikipedia (Merity et al., 2017), Fictional Stories (Forsythe, 2024), and BBC News (Li et al., 2024). These 300 texts are manually validated to have high quality and trimmed to 256 tokens. Of these, we select the first 32 tokens as context and keep the remaining 224 as the original continuation. Additionally, we create a 128-token scenario, where the model's first 96 tokens are compared to the first 96 tokens from the original continuation. For both length scenarios, we gather 3 annotations per comparison. All models generate using greedy decoding, besides the strong baselines that uses nucleus sampling with $TopP = 0.9$, $Temp = 0.7$ and $TopK = 50$. Examples of generated texts are available in Appendix C.2.

In Table 1 we report the percentage of times that a continuation was either preferred or judged equally good to the original. We also report the models' perplexity on the 32-token contexts and the TTR of the tokens in the continuation sequences. Since TTR is sensitive to length, we calculate this metric using the last 96 generated tokens for both the 128 and 256 token scenarios.

4.1 Text Generation Results

Hyperfitting drastically increases the human preference ratio. This is particularly true for the 256-token scenario, where the initially worst performing TinyLlama increases from 4.9% to 34.4%, putting it on par with Llama 3.1 70b. While all models perform worse on the 256 scenario, the drop is less drastic for hyperfitted models. Indeed, greedy decoding with hyperfitted models produce both higher human ratings, and a higher ttr when compared with their nucleus sampling counterparts—a method proposed specifically to mitigate repetitions. Citation blocked models see no noticeable drop in performance.

There is a clear correlation with the average TTR and human preference, as the hyperfitted models demonstrate a comparably small drop in both metrics as sequence length increases. Interestingly, all hyperfitted models perform abysmally in terms of perplexity, corroborating the lack of correlation between this metric and a model's ability to generate longer. This is discussed further in Section 5.

4.2 Diversity and Dataset Overlap

As hyperfitting is by definition overfitting a model on a tiny set of samples, we investigate how this impacts the model's diversity and overlap with the training dataset. For diversity between generated sequences we apply Self-BLEU, which measures the highest pairwise BLEU score for all pairwise

Table 2: Diversity metrics for generated texts of 96 tokens. Self-BLEU measures diversity within the generated set, while BLEU and Overlap are measured against the dataset. BLEU captures the highest score for any sequence of similar length, and Overlap denotes the longest matching sequence.

	Self-BLEU		Dataset BLEU		Dataset Overlap	
Model	**Avg**	**Max**	**Avg**	**Max**	**Avg**	**Max**
Original Models						
TinyLLama	1.5	96.8	2.0	10.0	4.2	9.0
DeepSeek	2.4	41.2	2.6	11.9	4.5	9.0
Llama 3.1	0.9	33.7	1.9	5.9	4.0	7.0
Hyperfitted Models						
TinyLlama	1.1	36.0	3.3	9.8	5.5	15.0
DeepSeek	1.4	26.2	3.9	18.6	5.7	40.0
Llama 3.1	1.0	13.5	3.6	32.1	5.8	37.0
Hyperfitted Models + Citation Blocking						
TinyLlama	1.1	31.4	3.2	9.8	4.9	8.0
DeepSeek	1.4	26.9	3.2	9.7	4.9	8.0
Llama 3.1	1.0	14.7	3.0	8.5	4.7	8.0

generated sequences; Dataset BLEU represents the maximum BLEU score between a generated sequence and any 96 token subsequence from the dataset; Dataset Overlap measures the longest overlapping subsequence between each generated sequence and the dataset.

For each metric we first calculate the highest score for each generated sequence separately, Table 2 then presents both the average and the maximum of these highest values[2]. In terms of Self-BLEU, the hyperfitted models, both with and without citation blocking, produce texts that are more diverse from one another than texts produced by the original models. As the original models are prone to repetitions, this may indicate that certain repetitive behaviors appear in multiple generated texts.

The distribution of longest overlaps are visualized in Figure 3, for an additional 1000 generated texts per model. From outliers in these distributions, and max values for Dataset BLEU, it is clear that the hyperfitted models occasionally fall back to re-citing from the training data if not blocked. However, considering that the majority of text overlaps are considerably shorter, such occurrences are rare. Indeed, less than 2% of the texts generated without blocking contain overlaps longer than 10 tokens, and the vast majority of overlaps fall in a range similar to that of the original models.

Considering that the average highest BLEU overlap is only a single point higher than the original models, an overwhelming majority of the generated texts do not simply repeat material from the training data. We therefore conclude that hyperfitting causes a generalizable increase in text generation capabilities. More details about the overlapping sequences are available in Appendix B.2. These experiments show that the hyperfitted TinyLLama is citation blocked more frequently compared to its larger counterpart, and that all models are more prone to repeating the dataset when generating from contexts in the fiction datasets.

[2]By calculating the highest value followed by the mean and max we attain more insightful and interpretable numbers. If one instead calculates the average directly this leads to extremely low numbers for all metrics.

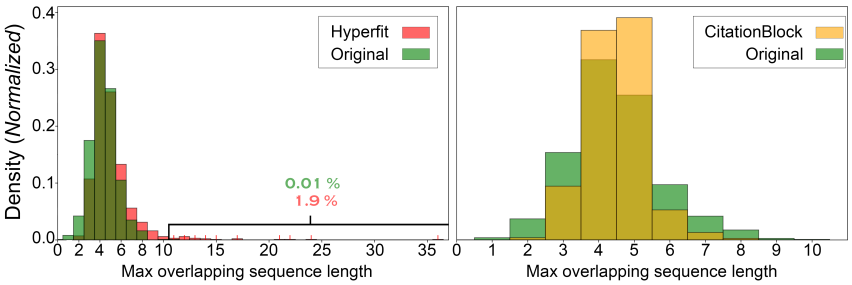

Figure 3: Distribution of the longest overlap between 1000 generated texts and the dataset

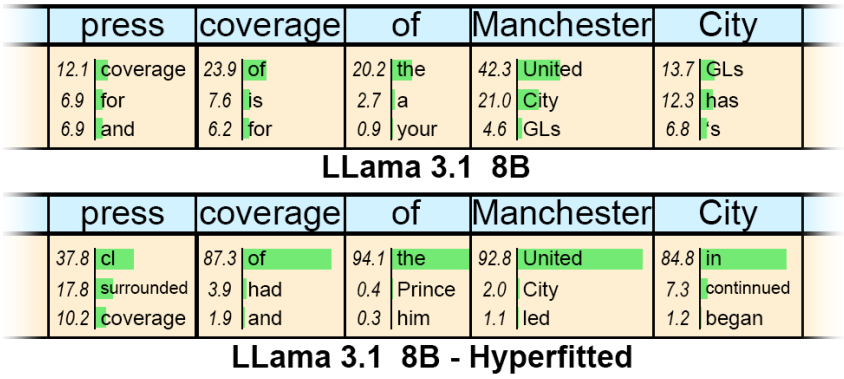

Figure 4: A subsequence from the validation data and the corresponding top-3 predictions. The words: "Coverage", "Manchester" and "United" never appear in the hyperfitting dataset.

5 Sharpened Predictions

Given the boost in textual quality brought about by hyperfitting, we investigate why hyperfitted models achieve such poor perplexity on held-out data. Using the 300 texts and their original continuations from the experiment reported in Section 4, we collect information on the predicted vocabulary distributions of different models. As we observe similar trends across all our hyperfitted models, the results in Table 3 display information only on a subset of the models.

The hyperfitted models exhibit significantly lower entropy in their predicted vocabulary distributions compared to the non-hyperfitted models. This entails that almost all of the probability mass is attributed to a single token. Given the poor perplexity on withheld texts, this sharpened prediction behavior persists even when these predictions are wrong. This persistence is exemplified in Figure 4, where the hyperfitted model assigns "United" a 92.8% probability, although it assigned the previous word "Manchester" a near 0 probability. Neither of these words occur in the hyperfitting dataset.

Hyperfitted models produce vocabulary predictions with extremely low entropy. Moreover, the low training loss indicates that almost all of the probability is consistently assigned to the correct next token during training. This sharpened prediction pattern is, to a degree, transferred to unseen data where the model continues to heavily favor certain candidates. When evaluating these predictions against the unseen data, the low-entropy predictions assign very low probability to words that occur in the new sequences but are not favored by the model, which in turn results in very high perplexity regardless of the quality of the texts they generate. It is worth noting here that, although we follow standard practice and report performance on held-out data using the exponentiated perplexity metric, the key point is really that predictions with low inherent entropy result in high cross-entropy when measured against unseen sequences.

Table 3: Distributions predicted for the original texts (context + continuation) in Section 4. @N indicating the accumulated probability of the N:th tokens with the highest probability.

Model	Perplexity	Entropy	@1 Prob	@3 Prob	@5 Prob
Original Models					
DeepSeek (7B)	12.7	3.48	49.1	67.3	73.9
Llama 3.1 (8B)	13.1	3.47	48.4	67.1	73.9
Llama 3.1 (70B)	9.7	2.84	56.2	73.7	79.5
Hyperfitted Models					
DeepSeek (7B)	94.7	1.32	74.5	90.0	93.3
Llama 3.1 (8B)	103	1.46	74.4	89.2	92.3

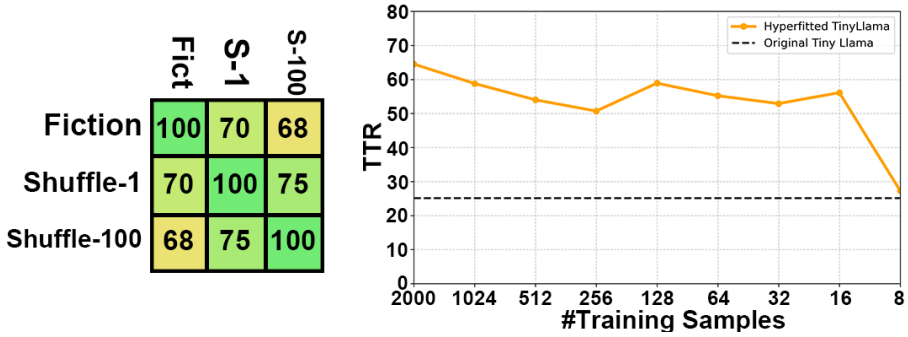

Figure 5: **Left**: Top-1 rank similarity matrix of Llama 3.1 (8B) hyperfitted on identical, but shuffled, data. **Right**: The resulting mean TTR of 300 generated texts as the number of training samples vary.

6 Data Influence

The following experiments aim to investigate the effect and importance of the data used during hyperfitting. For this endeavor we alter only the data used during hyperfitting and, unless stated otherwise, apply the same training procedure as Section 3. These experiments focus on a single property at a time and do not account for potential relationships between these properties.

6.1 Determinacy of Data

As an initial experiment, we evaluate the extent to which the set of training samples deterministically dictates the outcome of the hyperfitting process. To this end, we produce two additional versions of the fiction dataset: 'Shuffle-1' and 'Shuffle-All'. For Shuffle-1 the order of only two samples is switched, and for Shuffle-All dataset, the entire order is shuffled. For both datasets we hyperfit Llama 3.1 using the same fixed random seed as used in Section 3, meaning all models train on the same data, but in a different order.

Using the full original texts from Section 3, we calculate how often two models produce the same top-1 prediction. This is displayed in the left similarity matrix of Figure 5. All models differ in approximately 30% of their top rank predictions; this is a noticeably large difference from training on the same data. This is especially noteworthy considering that some portion of these predictions will be for subwords, which are almost guaranteed to have the same top rank. Conclusively, the data does not deterministically account for which tokens emerge as top candidates from the hyperfitting process.

6.2 Type of Data

Although Section 6.1 shows that data does not fully determine the resulting model, we nevertheless explore whether any trends emerge between the hyperfitting datasets and downstream dataset capabilities. Therefore, we additionally hyperfit Llama 3.1 with data from both Wikipedia and BBC News separately and measure per-dataset human preference for the 256-token task in Section 3. Qualitative examples of these models are available in Appendix C.2.

Table 4: Human success ratio for 256 token lengths across Fiction, Wiki, and News datasets.

Model	Fiction Pref	Wikipedia Pref	News Pref	Average
Original Models				
Llama 3.1 (8B)	21.9	26.0	24.8	24.23
Hyperfitted Models				
Llama 3.1 (8B) **Fiction**	41.0	40.4	40.8	40.73
Llama 3.1 (8B) **News**	59.3	77.2	62.6	66.37
Llama 3.1 (8B) **Wiki**	55.5	52.6	44.5	50.87

The results in Table 4 show that the difference in overall performance between these models is drastic. The news model performs best across all datasets, followed by the Wikipedia model. All of our hyperfitted models consistently outperform their original counterparts. However, no clear trend emerges between the types of training data and the performance on specific datasets. When factoring in the results of Section 6.1, we cannot draw any further conclusions regarding the type of training data and downstream capabilities.

6.3 Quantity of Data

Finally, we measure the effect of the number of training samples from the Fiction dataset when hyperfitting TinyLlama. To this end we keep the number of updates constant at 5000, entailing more epochs as the number of samples decreases. The right part of Figure 5 displays the resulting TTR of the first 96 tokens when greedily generating from the 300 contexts used in Section 4. Since human annotations are costly, TTR is intended as a crude estimate of quality by measuring the repetitiveness of generations. Further discussion regarding TTR as an automatic metric is available in Appendix A.1.

Although there is an initial decline in TTR when decreasing from 2000 samples, the TTR remains above 50 up until there are only 8 training samples. This means that in terms of producing less repetitive output, improvements may be seen from very few samples. Further, we note that 8 samples equals our hyperfitting batch size, meaning that at this point all batch updates are identical, and may hence be indicative of why this is drastically worse than 16 samples.

7 Hyperfitting and the Bigger Picture

7.1 Image Generation

To investigate the hyperfitting phenomenon for an additional modality, we hyperfit ImageGPT-Large (774M parameters) (Chen et al., 2020) on 2,000 randomly selected images from CIFAR-10. Besides using visual tokens, ImageGPT is a standard Transformer architecture and was pre-trained using next-token prediction on 32x32 images. Figure 6 contains a qualitative comparison of the greedy generation when the models receive the first 25% of an image. More details and results are available in Appendix B.4.

From visual inspection it is clear that the hyperfitted model produces higher quality images that more resemble actual objects and subjects (see Appendix B.4 for more examples). Although the generated image quality is unimpressive compared to contemporary diffusion based models, the relative improvement allows us to conclude that the hyperfitting phenomenon extends to other modalities beyond just text. Moreover, we note that greedily generating with ImageGPT results in repetitive patterns analogous to the repetitive texts of LLMs. This strongly indicates that the repetitive nature of Transformer LLMs is not an artifact of the repetitions found in natural language, as posed by Fu et al. (2020) and Holtzman et al. (2020).

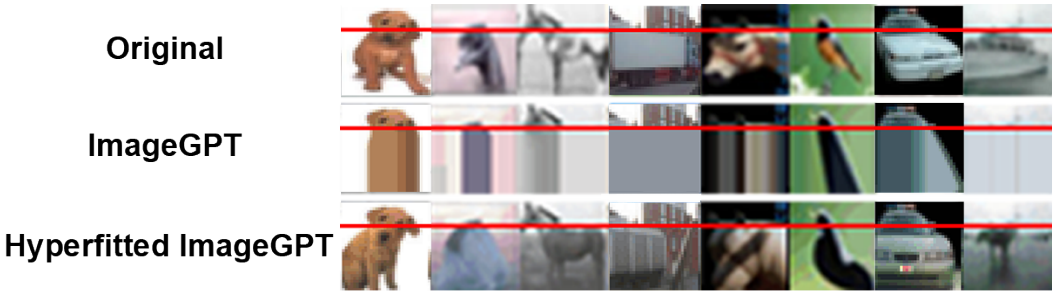

Figure 6: Examples of generated images using greedy decoding when passed 25% of an image.

7.2 Relationship to Grokking and Double Descent

The hyperfitting phenomenon differs in several key ways from the reported work on grokking and double descent. **(1)** As seen in Figure 2, the positive effect of hyperfitting occurs as training loss approaches zero. In contrast, previous phenomena occur during prolonged exposure to low training loss. **(2)** All our hyperfitted models are pre-trained LLMs with billions of parameters, whereas previous work utilizes comparably small and randomly initialized networks. **(3)** Hyperfitting is observed in the task of sequence generation, where the model's predictions are recursively added to its input. Previously observed phenomena have focused on single output tasks, such as classification and regression. **(4)** Hyperfitting sees improvements in terms of TTR after only a few epochs, as evident in Figure 2, significantly faster than the reported occurrence of double descent and the delayed rewards of grokking. **(5)** None of the hyperfitting training utilizes any form of weight decay, which is speculated to be a main contributor to delayed generalization in grokking (Liu et al., 2023).

From **(2)** and **(3)**, we conclude that hyperfitting is observed at a higher level of model and task complexity. One may argue that if grokking were to occur in large pre-trained models, it would happen quickly and would therefore reconcile **(1)** and **(4)**. However, this is yet to be achieved, and it is unclear if such speed would even be compatible with the slow progress of weight-decay **(5)**. Therefore, besides all phenomena seemingly contradicting early stopping, we currently find no evidence of a commonality. We therefore argue for treating hyperfitting as a separate phenomenon.

Finally, one may note that the validation loss for hyperfitting never decreases, distinguishing it from the hallmark of double descent and grokking. However, as the next-token prediction loss is not fully aligned with our task of sequence generation, we do not consider this to be a reasonable comparison. Admittedly, this entails we cannot track an aligned validation score, preventing us from proving that hyperfitting fundamentally differs from previous discoveries.

7.3 Top-Rank Encouragement Hypothesis

This subsection explores our observation that scenarios with low training loss cause desirable tokens to be ranked higher even when validation loss is poor. For this, we use the term 'top-ranks' to refer to the set of most probable tokens in a predicted distribution, and perplexity as the exponential of the log loss for the next token.[3] The notion of a "desirable" token entails that, if generated, the token would extend the current sequence in a manner acceptable by a human.

Since next-token prediction does not factor in the order and rank of predictions, we note that a higher loss leaves more room for undesired candidates to reside within the predicted top-ranks. In a scenario of moderate perplexity, this means that two models achieving identical perplexity on all time-steps, can still have different top-ranks. This notion is visualized in Figure 7.

A low training perplexity entails distributions during training with low entropy. As observed in Section 5, this entropy behaviour is transferred to validation data. But simply lowering entropy does not by itself entail that top-rank predictions improve. Indeed, we can freely modify the entropy of any (non-uniform) distribution by applying temperature to it, without any change in the predicted order. It follows that something additional happens to the model as it achieves a low training loss.

[3]Note again that the important point is not whether the loss is measured on an exponential scale or not, but that it is the cross-entropy with respect to an external sequence, as opposed to the inherent entropy of the predicted probability distribution.

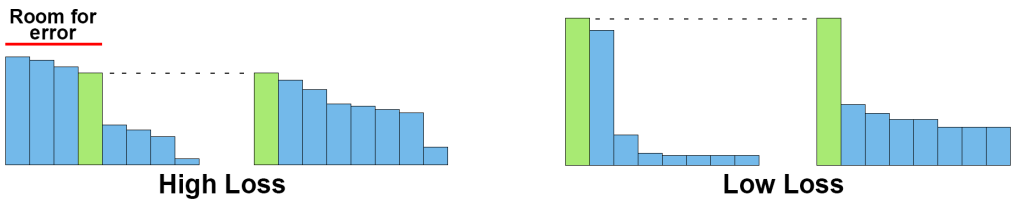

Figure 7: Visualization of how distributions with the same probability for the next token (visualized in green) leave more or less room for error in the top candidates, depending on their entropy.

We hypothesize that training scenarios where a model achieves a low loss teaches the model to prioritize desirable top-rank candidate. We refer to this as top-rank encouragement. Having a desirable token in the top-rank is distinctly different from perplexity, which measures the average probability of the next token over a set of sequences. Section 4 further demonstrates that a model can predict desirable top-rank tokens, despite poor perplexity on the context.

8 Discussion and Conclusions

We introduce the hyperfitting phenomenon: where pre-trained LLMs consistently see significant improvements in open-ended text generation by overfitting to a very small set of samples. The textual quality of the models are assessed via human verified English speakers, resulting in a new dataset with over 20,000 annotations. We provide extensive evidence that the hyperfitting phenomenon is reproducible across various model sizes, data types, and extends to autoregressive image generation. In all these scenarios, the hyperfitted models predict very sharp distributions, with the candidates seemingly emerging from knowledge acquired during pre-training.

For text generation, the hyperfitted models produce texts that are rated higher by human annotators. Interestingly, using greedy decoding with hyperfitted models results in less repetitive texts than using nucleus sampling with the original models. This showcases a key flaw in sampling-only methods: they doesn't change predicted probabilities, so while it reduces the chance of repetition, the risk still increases with longer sequences. Furthermore, we find that our hyperfitted models rarely repeat longer subsequences from the training data. Even when explicitly blocking all such subsequences, the models still produce high-quality texts.

We find that hyperfitting on the same data, but shuffled, results in a model with 30% different top-1 predictions. This indicates that the stochastic hyperfitting process itself is responsible for a large part of which top-1 candidates emerge. Additionally, we found no correlation between the training data and downstream generation capabilities. However, models hyperfitted on Wikipedia and BBC News outperform our model using fiction data. Due to these nuanced results, further work is needed to discern the impact of the data used during hyperfitting.

All our experiments (besides the nucleus sampling baseline in Section 4) are centered around greedy decoding. This is intended to remove as many elements of uncertainty as possible, and allow us to investigate the underlying model directly. Further investigation of combining hyperfitting with other sampling strategies and heuristics is left to future work. However, we note that sampling without any temperature may result in a near-deterministic generative behaviour, considering the sharp distributions of the hyperfitted models.

Finally, through our observations of the extreme scenario that hyperfitting poses, we hypothesize that the behavior of predicting good tokens in the top ranks is itself a learnable behavior. We refer to this as top-rank encouragement and speculate that it is more likely to occur in scenarios with low training loss. To what extent such a hypothesis is true, and why hyperfitting results in generative capabilities that generalize, are important open questions for future work.

Ethics Statement

The research reported in this paper involves an extensive human evaluation. In the interest of fairness as well as data quality, annotators were hired as freelancers through Fiverr[4] and paid 10 USD per hour of annotation.

[4]https://www.fiverr.com

REFERENCES

Gregor Bachmann and Vaishnavh Nagarajan. The pitfalls of next-token prediction, 2024. URL https://arxiv.org/abs/2403.06963.

Mikhail Belkin, Daniel Hsu, Siyuan Ma, and Soumik Mandal. Reconciling modern machine-learning practice and the classical bias–variance trade-off. Proceedings of the National Academy of Sciences, 116(32):15849–15854, July 2019. ISSN 1091-6490. doi: 10.1073/pnas.1903070116. URL http://dx.doi.org/10.1073/pnas.1903070116.

Xiao Bi, Deli Chen, Guanting Chen, Shanhuang Chen, Damai Dai, Chengqi Deng, Honghui Ding, Kai Dong, Qiushi Du, Zhe Fu, Huazuo Gao, Kaige Gao, Wenjun Gao, Ruiqi Ge, Kang Guan, Daya Guo, Jianzhong Guo, Guangbo Hao, Zhewen Hao, Ying He, Wenjie Hu, Panpan Huang, Erhang Li, Guowei Li, Jiashi Li, Yao Li, Y. K. Li, Wenfeng Liang, Fangyun Lin, A. X. Liu, Bo Liu, Wen Liu, Xiaodong Liu, Xin Liu, Yiyuan Liu, Haoyu Lu, Shanghao Lu, Fuli Luo, Shirong Ma, Xiaotao Nie, Tian Pei, Yishi Piao, Junjie Qiu, Hui Qu, Tongzheng Ren, Zehui Ren, Chong Ruan, Zhangli Sha, Zhihong Shao, Junxiao Song, Xuecheng Su, Jingxiang Sun, Yaofeng Sun, Minghui Tang, Bingxuan Wang, Peiyi Wang, Shiyu Wang, Yaohui Wang, Yongji Wang, Tong Wu, Y. Wu, Xin Xie, Zhenda Xie, Ziwei Xie, Yiliang Xiong, Hanwei Xu, R. X. Xu, Yanhong Xu, Dejian Yang, Yuxiang You, Shuiping Yu, Xingkai Yu, B. Zhang, Haowei Zhang, Lecong Zhang, Liyue Zhang, Mingchuan Zhang, Minghua Zhang, Wentao Zhang, Yichao Zhang, Chenggang Zhao, Yao Zhao, Shangyan Zhou, Shunfeng Zhou, Qihao Zhu, and Yuheng Zou. Deepseek llm: Scaling open-source language models with longtermism. CoRR, abs/2401.02954, 2024. URL https://arxiv.org/abs/2401.02954.

Tom B. Brown, Benjamin Mann, Nick Ryder, Melanie Subbiah, Jared Kaplan, Prafulla Dhariwal, Arvind Neelakantan, Pranav Shyam, Girish Sastry, Amanda Askell, Sandhini Agarwal, Ariel Herbert-Voss, Gretchen Krueger, Tom Henighan, Rewon Child, Aditya Ramesh, Daniel M. Ziegler, Jeff Wu, Clemens Winter, Christopher Hesse, Mark Chen, Eric Sigler, Ma teusz Litwin, Scott Gray, Benjamin Chess, Jack Clark, Christopher Berner, Sam McCandlish, Alec Radford, Ilya Sutskever, and Dario Amodei. Language models are few-shot learners. ArXiv, abs/2005.14165, 2020. URL https://api.semanticscholar.org/CorpusID:218971783.

Sébastien Bubeck, Varun Chandrasekaran, Ronen Eldan, Johannes Gehrke, Eric Horvitz, Ece Kamar, Peter Lee, Yin Tat Lee, Yuanzhi Li, Scott M. Lundberg, Harsha Nori, Hamid Palangi, Marco Túlio Ribeiro, and Yi Zhang. Sparks of artificial general intelligence: Early experiments with GPT-4. CoRR, abs/2303.12712, 2023. doi: 10.48550/ARXIV.2303.12712. URL https://doi.org/10.48550/arXiv.2303.12712.

Fredrik Carlsson, Johan Broberg, Erik Hillbom, Magnus Sahlgren, and Joakim Nivre. Branch-GAN: Improving text generation with (not so) large language models. In The Twelfth International Conference on Learning Representations, 2024. URL https://openreview.net/forum?id=sHEJJmzBIN.

Mark Chen, Alec Radford, Rewon Child, Jeffrey Wu, Heewoo Jun, David Luan, and Ilya Sutskever. Generative pretraining from pixels. In International conference on machine learning, pp. 1691–1703. PMLR, 2020.

Abhimanyu Dubey, Abhinav Jauhri, Abhinav Pandey, Abhishek Kadian, Ahmad Al-Dahle, Aiesha Letman, Akhil Mathur, Alan Schelten, Amy Yang, Angela Fan, Anirudh Goyal, Anthony Hartshorn, Aobo Yang, Archi Mitra, Archie Sravankumar, Artem Korenev, Arthur Hinsvark, Arun Rao, Aston Zhang, Aurelien Rodriguez, Austen Gregerson, Ava Spataru, Baptiste Roziere, Bethany Biron, Binh Tang, Bobbie Chern, Charlotte Caucheteux, Chaya Nayak, Chloe Bi, Chris Marra, Chris McConnell, Christian Keller, Christophe Touret, Chunyang Wu, Corinne Wong, Cristian Canton Ferrer, Cyrus Nikolaidis, Damien Allonsius, Daniel Song, Danielle Pintz, Danny Livshits, David Esiobu, Dhruv Choudhary, Dhruv Mahajan, Diego Garcia-Olano, Diego Perino, Dieuwke Hupkes, Egor Lakomkin, Ehab AlBadawy, Elina Lobanova, Emily Dinan, Eric Michael Smith, Filip Radenovic, Frank Zhang, Gabriel Synnaeve, Gabrielle Lee, Georgia Lewis Anderson, Graeme Nail, Gregoire Mialon, Guan Pang, Guillem Cucurell, Hailey Nguyen, Hannah Korevaar, Hu Xu, Hugo Touvron, Iliyan Zarov, Imanol Arrieta Ibarra, Isabel Kloumann, Ishan

Misra, Ivan Evtimov, Jade Copet, Jaewon Lee, Jan Geffert, Jana Vranes, Jason Park, Jay Mahadeokar, Jeet Shah, Jelmer van der Linde, Jennifer Billock, Jenny Hong, Jenya Lee, Jeremy Fu, Jianfeng Chi, Jianyu Huang, Jiawen Liu, Jie Wang, Jiecao Yu, Joanna Bitton, Joe Spisak, Jongsoo Park, Joseph Rocca, Joshua Johnstun, Joshua Saxe, Junteng Jia, Kalyan Vasuden Alwala, Kartikeya Upasani, Kate Plawiak, Ke Li, Kenneth Heafield, Kevin Stone, Khalid El-Arini, Krithika Iyer, Kshitiz Malik, Kuenley Chiu, Kunal Bhalla, Lauren Rantala-Yeary, Laurens van der Maaten, Lawrence Chen, Liang Tan, Liz Jenkins, Louis Martin, Lovish Madaan, Lubo Malo, Lukas Blecher, Lukas Landzaat, Luke de Oliveira, Madeline Muzzi, Mahesh Pasupuleti, Mannat Singh, Manohar Paluri, Marcin Kardas, Mathew Oldham, Mathieu Rita, Maya Pavlova, Melanie Kambadur, Mike Lewis, Min Si, Mitesh Kumar Singh, Mona Hassan, Naman Goyal, Narjes Torabi, Nikolay Bashlykov, Nikolay Bogoychev, Niladri Chatterji, Olivier Duchenne, Onur Çelebi, Patrick Alrassy, Pengchuan Zhang, Pengwei Li, Petar Vasic, Peter Weng, Prajjwal Bhargava, Pratik Dubal, Praveen Krishnan, Punit Singh Koura, Puxin Xu, Qing He, Qingxiao Dong, Ragavan Srinivasan, Raj Ganapathy, Ramon Calderer, Ricardo Silveira Cabral, Robert Stojnic, Roberta Raileanu, Rohit Girdhar, Rohit Patel, Romain Sauvestre, Ronnie Polidoro, Roshan Sumbaly, Ross Taylor, Ruan Silva, Rui Hou, Rui Wang, Saghar Hosseini, Sahana Chennabasappa, Sanjay Singh, Sean Bell, Seohyun Sonia Kim, Sergey Edunov, Shaoliang Nie, Sharan Narang, Sharath Raparthy, Sheng Shen, Shengye Wan, Shruti Bhosale, Shun Zhang, Simon Vandenhende, Soumya Batra, Spencer Whitman, Sten Sootla, Stephane Collot, Suchin Gururangan, Sydney Borodinsky, Tamar Herman, Tara Fowler, Tarek Sheasha, Thomas Georgiou, Thomas Scialom, Tobias Speckbacher, Todor Mihaylov, Tong Xiao, Ujjwal Karn, Vedanuj Goswami, Vibhor Gupta, Vignesh Ramanathan, Viktor Kerkez, Vincent Gonguet, Virginie Do, Vish Vogeti, Vladan Petrovic, Weiwei Chu, Wenhan Xiong, Wenyin Fu, Whitney Meers, Xavier Martinet, Xiaodong Wang, Xiaoqing Ellen Tan, Xinfeng Xie, Xuchao Jia, Xuewei Wang, Yaelle Goldschlag, Yashesh Gaur, Yasmine Babaei, Yi Wen, Yiwen Song, Yuchen Zhang, Yue Li, Yuning Mao, Zacharie Delpierre Coudert, Zheng Yan, Zhengxing Chen, Zoe Papakipos, Aaditya Singh, Aaron Grattafiori, Abha Jain, Adam Kelsey, Adam Shajnfeld, Adithya Gangidi, Adolfo Victoria, Ahuva Goldstand, Ajay Menon, Ajay Sharma, Alex Boesenberg, Alex Vaughan, Alexei Baevski, Allie Feinstein, Amanda Kallet, Amit Sangani, Anam Yunus, Andrei Lupu, Andres Alvarado, Andrew Caples, Andrew Gu, Andrew Ho, Andrew Poulton, Andrew Ryan, Ankit Ramchandani, Annie Franco, Aparajita Saraf, Arkabandhu Chowdhury, Ashley Gabriel, Ashwin Bharambe, Assaf Eisenman, Azadeh Yazdan, Beau James, Ben Maurer, Benjamin Leonhardi, Bernie Huang, Beth Loyd, Beto De Paola, Bhargavi Paranjape, Bing Liu, Bo Wu, Boyu Ni, Braden Hancock, Bram Wasti, Brandon Spence, Brani Stojkovic, Brian Gamido, Britt Montalvo, Carl Parker, Carly Burton, Catalina Mejia, Changhan Wang, Changkyu Kim, Chao Zhou, Chester Hu, Ching-Hsiang Chu, Chris Cai, Chris Tindal, Christoph Feichtenhofer, Damon Civin, Dana Beaty, Daniel Kreymer, Daniel Li, Danny Wyatt, David Adkins, David Xu, Davide Testuggine, Delia David, Devi Parikh, Diana Liskovich, Didem Foss, Dingkang Wang, Duc Le, Dustin Holland, Edward Dowling, Eissa Jamil, Elaine Montgomery, Eleonora Presani, Emily Hahn, Emily Wood, Erik Brinkman, Esteban Arcaute, Evan Dunbar, Evan Smothers, Fei Sun, Felix Kreuk, Feng Tian, Firat Ozgenel, Francesco Caggioni, Francisco Guzmán, Frank Kanayet, Frank Seide, Gabriela Medina Florez, Gabriella Schwarz, Gada Badeer, Georgia Swee, Gil Halpern, Govind Thattai, Grant Herman, Grigory Sizov, Guangyi, Zhang, Guna Lakshminarayanan, Hamid Shojanazeri, Han Zou, Hannah Wang, Hanwen Zha, Haroun Habeeb, Harrison Rudolph, Helen Suk, Henry Aspegren, Hunter Goldman, Ibrahim Damlaj, Igor Molybog, Igor Tufanov, Irina-Elena Veliche, Itai Gat, Jake Weissman, James Geboski, James Kohli, Japhet Asher, Jean-Baptiste Gaya, Jeff Marcus, Jeff Tang, Jennifer Chan, Jenny Zhen, Jeremy Reizenstein, Jeremy Teboul, Jessica Zhong, Jian Jin, Jingyi Yang, Joe Cummings, Jon Carvill, Jon Shepard, Jonathan McPhie, Jonathan Torres, Josh Ginsburg, Junjie Wang, Kai Wu, Kam Hou U, Karan Saxena, Karthik Prasad, Kartikay Khandelwal, Katayoun Zand, Kathy Matosich, Kaushik Veeraraghavan, Kelly Michelena, Keqian Li, Kun Huang, Kunal Chawla, Kushal Lakhotia, Kyle Huang, Lailin Chen, Lakshya Garg, Lavender A, Leandro Silva, Lee Bell, Lei Zhang, Liangpeng Guo, Licheng Yu, Liron Moshkovich, Luca Wehrstedt, Madian Khabsa, Manav Avalani, Manish Bhatt, Maria Tsimpoukelli, Martynas Mankus, Matan Hasson, Matthew Lennie, Matthias Reso, Maxim Groshev, Maxim Naumov, Maya Lathi, Meghan Keneally, Michael L. Seltzer, Michal Valko, Michelle Restrepo, Mihir Patel, Mik Vyatskov, Mikayel Samvelyan, Mike Clark, Mike Macey, Mike Wang, Miquel Jubert Hermoso, Mo Metanat, Mohammad Rastegari, Munish Bansal, Nandhini Santhanam, Natascha Parks, Natasha White, Navyata Bawa, Nayan Singhal, Nick Egebo, Nicolas Usunier, Nikolay Pavlovich Laptev, Ning Dong, Ning Zhang, Norman Cheng, Oleg Chernoguz, Olivia Hart, Omkar Salpekar, Ozlem Kalinli,

Parkin Kent, Parth Parekh, Paul Saab, Pavan Balaji, Pedro Rittner, Philip Bontrager, Pierre Roux, Piotr Dollar, Polina Zvyagina, Prashant Ratanchandani, Pritish Yuvraj, Qian Liang, Rachad Alao, Rachel Rodriguez, Rafi Ayub, Raghotham Murthy, Raghu Nayani, Rahul Mitra, Raymond Li, Rebekkah Hogan, Robin Battey, Rocky Wang, Rohan Maheswari, Russ Howes, Ruty Rinott, Sai Jayesh Bondu, Samyak Datta, Sara Chugh, Sara Hunt, Sargun Dhillon, Sasha Sidorov, Satadru Pan, Saurabh Verma, Seiji Yamamoto, Sharadh Ramaswamy, Shaun Lindsay, Shaun Lindsay, Sheng Feng, Shenghao Lin, Shengxin Cindy Zha, Shiva Shankar, Shuqiang Zhang, Shuqiang Zhang, Sinong Wang, Sneha Agarwal, Soji Sajuyigbe, Soumith Chintala, Stephanie Max, Stephen Chen, Steve Kehoe, Steve Satterfield, Sudarshan Govindaprasad, Sumit Gupta, Sungmin Cho, Sunny Virk, Suraj Subramanian, Sy Choudhury, Sydney Goldman, Tal Remez, Tamar Glaser, Tamara Best, Thilo Kohler, Thomas Robinson, Tianhe Li, Tianjun Zhang, Tim Matthews, Timothy Chou, Tzook Shaked, Varun Vontimitta, Victoria Ajayi, Victoria Montanez, Vijai Mohan, Vinay Satish Kumar, Vishal Mangla, Vítor Albiero, Vlad Ionescu, Vlad Poenaru, Vlad Tiberiu Mihailescu, Vladimir Ivanov, Wei Li, Wenchen Wang, Wenwen Jiang, Wes Bouaziz, Will Constable, Xiaocheng Tang, Xiaofang Wang, Xiaojian Wu, Xiaolan Wang, Xide Xia, Xilun Wu, Xinbo Gao, Yanjun Chen, Ye Hu, Ye Jia, Ye Qi, Yenda Li, Yilin Zhang, Ying Zhang, Yossi Adi, Youngjin Nam, Yu, Wang, Yuchen Hao, Yundi Qian, Yuzi He, Zach Rait, Zachary DeVito, Zef Rosnbrick, Zhaoduo Wen, Zhenyu Yang, and Zhiwei Zhao. The Llama 3 herd of models. CoRR, abs/2407.21783, 2024. URL https://arxiv.org/abs/2407.21783.

Alasdair Forsythe. Text english code fiction nonfiction dataset, 2024. URL https://huggingface.co/datasets/alasdairforsythe/text-english-code-fiction-nonfiction. Accessed: 2024-09-30.

Zihao Fu, Wai Lam, Anthony Man-Cho So, and Bei Shi. A theoretical analysis of the repetition problem in text generation. In AAAI Conference on Artificial Intelligence, 2020. URL https://api.semanticscholar.org/CorpusID:229923515.

Daya Guo, Qihao Zhu, Dejian Yang, Zhenda Xie, Kai Dong, Wentao Zhang, Guanting Chen, Xiao Bi, Y. Wu, Y. K. Li, Fuli Luo, Yingfei Xiong, and Wenfeng Liang. Deepseek-coder: When the large language model meets programming – the rise of code intelligence, 2024. URL https://arxiv.org/abs/2401.14196.

Kaiming He, Xiangyu Zhang, Shaoqing Ren, and Jian Sun. Identity mappings in deep residual networks. In Bastian Leibe, Jiri Matas, Nicu Sebe, and Max Welling (eds.), Computer Vision – ECCV 2016, pp. 630–645, Cham, 2016. Springer International Publishing. ISBN 978-3-319-46493-0.

Dan Hendrycks, Collin Burns, Steven Basart, Andy Zou, Mantas Mazeika, Dawn Song, and Jacob Steinhardt. Measuring massive multitask language understanding. In International Conference on Learning Representations, 2021. URL https://openreview.net/forum?id=d7KBjmI3GmQ.

Ari Holtzman, Jan Buys, Li Du, Maxwell Forbes, and Yejin Choi. The curious case of neural text degeneration. In International Conference on Learning Representations, 2020. URL https://openreview.net/forum?id=rygGQyrFvH.

Nitish Shirish Keskar, Bryan McCann, Lav R. Varshney, Caiming Xiong, and Richard Socher. Ctrl: A conditional transformer language model for controllable generation. ArXiv, abs/1909.05858, 2019. URL https://api.semanticscholar.org/CorpusID:202573071.

Yucheng Li, Frank Guerin, and Chenghua Lin. Latesteval: Addressing data contamination in language model evaluation through dynamic and time-sensitive test construction. In Proceedings of the AAAI Conference on Artificial Intelligence, volume 38, pp. 18600–18607, 2024.

Ziming Liu, Eric J. Michaud, and Max Tegmark. Omnigrok: Grokking beyond algorithmic data, 2023. URL https://arxiv.org/abs/2210.01117.

Anton Lozhkov, Raymond Li, Loubna Ben Allal, Federico Cassano, Joel Lamy-Poirier, Nouamane Tazi, Ao Tang, Dmytro Pykhtar, Jiawei Liu, Yuxiang Wei, Tianyang Liu, Max Tian, Denis Kocetkov, Arthur Zucker, Younes Belkada, Zijian Wang, Qian Liu, Dmitry Abulkhanov, Indraneil Paul, Zhuang Li, Wen-Ding Li, Megan Risdal, Jia Li, Jian Zhu, Terry Yue Zhuo,

Evgenii Zheltonozhskii, Nii Osae Osae Dade, Wenhao Yu, Lucas Krauß, Naman Jain, Yixuan Su, Xuanli He, Manan Dey, Edoardo Abati, Yekun Chai, Niklas Muennighoff, Xiangru Tang, Muhtasham Oblokulov, Christopher Akiki, Marc Marone, Chenghao Mou, Mayank Mishra, Alex Gu, Binyuan Hui, Tri Dao, Armel Zebaze, Olivier Dehaene, Nicolas Patry, Canwen Xu, Julian McAuley, Han Hu, Torsten Scholak, Sebastien Paquet, Jennifer Robinson, Carolyn Jane Anderson, Nicolas Chapados, Mostofa Patwary, Nima Tajbakhsh, Yacine Jernite, Carlos Muñoz Ferrandis, Lingming Zhang, Sean Hughes, Thomas Wolf, Arjun Guha, Leandro von Werra, and Harm de Vries. Starcoder 2 and the stack v2: The next generation, 2024. URL https://arxiv.org/abs/2402.19173.

Clara Meister and Ryan Cotterell. Language model evaluation beyond perplexity. In Chengqing Zong, Fei Xia, Wenjie Li, and Roberto Navigli (eds.), Proceedings of the 59th Annual Meeting of the Association for Computational Linguistics and the 11th International Joint Conference on Natural Language Processing (Volume 1: Long Papers), pp. 5328–5339, Online, August 2021. Association for Computational Linguistics. doi: 10.18653/v1/2021.acl-long.414. URL https://aclanthology.org/2021.acl-long.414.

Stephen Merity, Caiming Xiong, James Bradbury, and Richard Socher. Pointer sentinel mixture models. In 5th International Conference on Learning Representations, ICLR 2017, Toulon, France, April 24-26, 2017, Conference Track Proceedings. OpenReview.net, 2017. URL https://openreview.net/forum?id=Byj72udxe.

Preetum Nakkiran, Gal Kaplun, Yamini Bansal, Tristan Yang, Boaz Barak, and Ilya Sutskever. Deep double descent: Where bigger models and more data hurt. In International Conference on Learning Representations, 2020. URL https://openreview.net/forum?id=B1g5sA4twr.

Long Ouyang, Jeff Wu, Xu Jiang, Diogo Almeida, Carroll L. Wainwright, Pamela Mishkin, Chong Zhang, Sandhini Agarwal, Katarina Slama, Alex Ray, John Schulman, Jacob Hilton, Fraser Kelton, Luke Miller, Maddie Simens, Amanda Askell, Peter Welinder, Paul Christiano, Jan Leike, and Ryan Lowe. Training language models to follow instructions with human feedback, 2022. URL https://arxiv.org/abs/2203.02155.

Alethea Power, Yuri Burda, Harri Edwards, Igor Babuschkin, and Vedant Misra. Grokking: Generalization beyond overfitting on small algorithmic datasets, 2022. URL https://arxiv.org/abs/2201.02177.

Aarohi Srivastava, Abhinav Rastogi, Abhishek Rao, Abu Awal Md Shoeb, Abubakar Abid, Adam Fisch, Adam R. Brown, Adam Santoro, Aditya Gupta, Adrià Garriga-Alonso, Agnieszka Kluska, Aitor Lewkowycz, Akshat Agarwal, Alethea Power, Alex Ray, Alex Warstadt, Alexander W. Kocurek, Ali Safaya, Ali Tazarv, Alice Xiang, Alicia Parrish, Allen Nie, Aman Hussain, Amanda Askell, Amanda Dsouza, Ambrose Slone, Ameet Rahane, Anantharaman S. Iyer, Anders Johan Andreassen, Andrea Madotto, Andrea Santilli, Andreas Stuhlmüller, Andrew M. Dai, Andrew La, Andrew Lampinen, Andy Zou, Angela Jiang, Angelica Chen, Anh Vuong, Animesh Gupta, Anna Gottardi, Antonio Norelli, Anu Venkatesh, Arash Gholamidavoodi, Arfa Tabassum, Arul Menezes, Arun Kirubarajan, Asher Mullokandov, Ashish Sabharwal, Austin Herrick, Avia Efrat, Aykut Erdem, Ayla Karakaş, B. Ryan Roberts, Bao Sheng Loe, Barret Zoph, Bartłomiej Bojanowski, Batuhan Özyurt, Behnam Hedayatnia, Behnam Neyshabur, Benjamin Inden, Benno Stein, Berk Ekmekci, Bill Yuchen Lin, Blake Howald, Bryan Orinion, Cameron Diao, Cameron Dour, Catherine Stinson, Cedrick Argueta, Cesar Ferri, Chandan Singh, Charles Rathkopf, Chenlin Meng, Chitta Baral, Chiyu Wu, Chris Callison-Burch, Christopher Waites, Christian Voigt, Christopher D Manning, Christopher Potts, Cindy Ramirez, Clara E. Rivera, Clemencia Siro, Colin Raffel, Courtney Ashcraft, Cristina Garbacea, Damien Sileo, Dan Garrette, Dan Hendrycks, Dan Kilman, Dan Roth, C. Daniel Freeman, Daniel Khashabi, Daniel Levy, Daniel Moseguí González, Danielle Perszyk, Danny Hernandez, Danqi Chen, Daphne Ippolito, Dar Gilboa, David Dohan, David Drakard, David Jurgens, Debajyoti Datta, Deep Ganguli, Denis Emelin, Denis Kleyko, Deniz Yuret, Derek Chen, Derek Tam, Dieuwke Hupkes, Diganta Misra, Dilyar Buzan, Dimitri Coelho Mollo, Diyi Yang, Dong-Ho Lee, Dylan Schrader, Ekaterina Shutova, Ekin Dogus Cubuk, Elad Segal, Eleanor Hagerman, Elizabeth Barnes, Elizabeth Donoway, Ellie Pavlick, Emanuele Rodolà, Emma Lam, Eric Chu, Eric Tang, Erkut Erdem, Ernie Chang,

Ethan A Chi, Ethan Dyer, Ethan Jerzak, Ethan Kim, Eunice Engefu Manyasi, Evgenii Zheltonozhskii, Fanyue Xia, Fatemeh Siar, Fernando Martínez-Plumed, Francesca Happé, Francois Chollet, Frieda Rong, Gaurav Mishra, Genta Indra Winata, Gerard de Melo, Germán Kruszewski, Giambattista Parascandolo, Giorgio Mariani, Gloria Xinyue Wang, Gonzalo Jaimovitch-Lopez, Gregor Betz, Guy Gur-Ari, Hana Galijasevic, Hannah Kim, Hannah Rashkin, Hannaneh Hajishirzi, Harsh Mehta, Hayden Bogar, Henry Francis Anthony Shevlin, Hinrich Schuetze, Hiromu Yakura, Hongming Zhang, Hugh Mee Wong, Ian Ng, Isaac Noble, Jaap Jumelet, Jack Geissinger, Jackson Kernion, Jacob Hilton, Jaehoon Lee, Jaime Fernández Fisac, James B Simon, James Koppel, James Zheng, James Zou, Jan Kocon, Jana Thompson, Janelle Wingfield, Jared Kaplan, Jarema Radom, Jascha Sohl-Dickstein, Jason Phang, Jason Wei, Jason Yosinski, Jekaterina Novikova, Jelle Bosscher, Jennifer Marsh, Jeremy Kim, Jeroen Taal, Jesse Engel, Jesujoba Alabi, Jiacheng Xu, Jiaming Song, Jillian Tang, Joan Waweru, John Burden, John Miller, John U. Balis, Jonathan Batchelder, Jonathan Berant, Jörg Frohberg, Jos Rozen, Jose Hernandez-Orallo, Joseph Boudeman, Joseph Guerr, Joseph Jones, Joshua B. Tenenbaum, Joshua S. Rule, Joyce Chua, Kamil Kanclerz, Karen Livescu, Karl Krauth, Karthik Gopalakrishnan, Katerina Ignatyeva, Katja Markert, Kaustubh Dhole, Kevin Gimpel, Kevin Omondi, Kory Wallace Mathewson, Kristen Chiafullo, Ksenia Shkaruta, Kumar Shridhar, Kyle McDonell, Kyle Richardson, Laria Reynolds, Leo Gao, Li Zhang, Liam Dugan, Lianhui Qin, Lidia Contreras-Ochando, Louis-Philippe Morency, Luca Moschella, Lucas Lam, Lucy Noble, Ludwig Schmidt, Luheng He, Luis Oliveros-Colón, Luke Metz, Lütfi Kerem Senel, Maarten Bosma, Maarten Sap, Maartje Ter Hoeve, Maheen Farooqi, Manaal Faruqui, Mantas Mazeika, Marco Baturan, Marco Marelli, Marco Maru, Maria Jose Ramirez-Quintana, Marie Tolkiehn, Mario Giulianelli, Martha Lewis, Martin Potthast, Matthew L Leavitt, Matthias Hagen, Mátyás Schubert, Medina Orduna Baitemirova, Melody Arnaud, Melvin McElrath, Michael Andrew Yee, Michael Cohen, Michael Gu, Michael Ivanitskiy, Michael Starritt, Michael Strube, Michał Swędrowski, Michele Bevilacqua, Michihiro Yasunaga, Mihir Kale, Mike Cain, Mimee Xu, Mirac Suzgun, Mitch Walker, Mo Tiwari, Mohit Bansal, Moin Aminnaseri, Mor Geva, Mozhdeh Gheini, Mukund Varma T, Nanyun Peng, Nathan Andrew Chi, Nayeon Lee, Neta Gur-Ari Krakover, Nicholas Cameron, Nicholas Roberts, Nick Doiron, Nicole Martinez, Nikita Nangia, Niklas Deckers, Niklas Muennighoff, Nitish Shirish Keskar, Niveditha S. Iyer, Noah Constant, Noah Fiedel, Nuan Wen, Oliver Zhang, Omar Agha, Omar Elbaghdadi, Omer Levy, Owain Evans, Pablo Antonio Moreno Casares, Parth Doshi, Pascale Fung, Paul Pu Liang, Paul Vicol, Pegah Alipoormolabashi, Peiyuan Liao, Percy Liang, Peter W Chang, Peter Eckersley, Phu Mon Htut, Pinyu Hwang, Piotr Miłkowski, Piyush Patil, Pouya Pezeshkpour, Priti Oli, Qiaozhu Mei, Qing Lyu, Qinlang Chen, Rabin Banjade, Rachel Etta Rudolph, Raefer Gabriel, Rahel Habacker, Ramon Risco, Raphaël Millière, Rhythm Garg, Richard Barnes, Rif A. Saurous, Riku Arakawa, Robbe Raymaekers, Robert Frank, Rohan Sikand, Roman Novak, Roman Sitelew, Ronan Le Bras, Rosanne Liu, Rowan Jacobs, Rui Zhang, Russ Salakhutdinov, Ryan Andrew Chi, Seungjae Ryan Lee, Ryan Stovall, Ryan Teehan, Rylan Yang, Sahib Singh, Saif M. Mohammad, Sajant Anand, Sam Dillavou, Sam Shleifer, Sam Wiseman, Samuel Gruetter, Samuel R. Bowman, Samuel Stern Schoenholz, Sanghyun Han, Sanjeev Kwatra, Sarah A. Rous, Sarik Ghazarian, Sayan Ghosh, Sean Casey, Sebastian Bischoff, Sebastian Gehrmann, Sebastian Schuster, Sepideh Sadeghi, Shadi Hamdan, Sharon Zhou, Shashank Srivastava, Sherry Shi, Shikhar Singh, Shima Asaadi, Shixiang Shane Gu, Shubh Pachchigar, Shubham Toshniwal, Shyam Upadhyay, Shyamolima Shammie Debnath, Siamak Shakeri, Simon Thormeyer, Simone Melzi, Siva Reddy, Sneha Priscilla Makini, Soo-Hwan Lee, Spencer Torene, Sriharsha Hatwar, Stanislas Dehaene, Stefan Divic, Stefano Ermon, Stella Biderman, Stephanie Lin, Stephen Prasad, Steven Piantadosi, Stuart Shieber, Summer Misherghi, Svetlana Kiritchenko, Swaroop Mishra, Tal Linzen, Tal Schuster, Tao Li, Tao Yu, Tariq Ali, Tatsunori Hashimoto, Te-Lin Wu, Théo Desbordes, Theodore Rothschild, Thomas Phan, Tianle Wang, Tiberius Nkinyili, Timo Schick, Timofei Kornev, Titus Tunduny, Tobias Gerstenberg, Trenton Chang, Trishala Neeraj, Tushar Khot, Tyler Shultz, Uri Shaham, Vedant Misra, Vera Demberg, Victoria Nyamai, Vikas Raunak, Vinay Venkatesh Ramasesh, vinay uday prabhu, Vishakh Padmakumar, Vivek Srikumar, William Fedus, William Saunders, William Zhang, Wout Vossen, Xiang Ren, Xiaoyu Tong, Xinran Zhao, Xinyi Wu, Xudong Shen, Yadollah Yaghoobzadeh, Yair Lakretz, Yangqiu Song, Yasaman Bahri, Yejin Choi, Yichi Yang, Yiding Hao, Yifu Chen, Yonatan Belinkov, Yu Hou, Yufang Hou, Yuntao Bai, Zachary Seid, Zhuoye Zhao, Zijian Wang, Zijie J. Wang, Zirui Wang, and Ziyi Wu. Beyond the imitation game: Quantifying and extrapolating the capabilities of language models. Transactions on Machine Learning Research, 2023. ISSN 2835-8856. URL https://openreview.net/forum?id=uyTL5Bvosj.

Alex Wang, Amanpreet Singh, Julian Michael, Felix Hill, Omer Levy, and Samuel R Bowman. Glue: A multi-task benchmark and analysis platform for natural language understanding. EMNLP 2018, pp. 353, 2018.

Jason Wei, Yi Tay, Rishi Bommasani, Colin Raffel, Barret Zoph, Sebastian Borgeaud, Dani Yogatama, Maarten Bosma, Denny Zhou, Donald Metzler, Ed H. Chi, Tatsunori Hashimoto, Oriol Vinyals, Percy Liang, Jeff Dean, and William Fedus. Emergent abilities of large language models. Transactions on Machine Learning Research, 2022a. ISSN 2835-8856. URL https://openreview.net/forum?id=yzkSU5zdwD. Survey Certification.

Jason Wei, Yi Tay, Rishi Bommasani, Colin Raffel, Barret Zoph, Sebastian Borgeaud, Dani Yogatama, Maarten Bosma, Denny Zhou, Donald Metzler, et al. Emergent abilities of large language models. Transactions on Machine Learning Research, 2022b.

Sean Welleck, Ilia Kulikov, Stephen Roller, Emily Dinan, Kyunghyun Cho, and Jason Weston. Neural text generation with unlikelihood training. CoRR, abs/1908.04319, 2019. URL http://arxiv.org/abs/1908.04319.

Jin Xu, Xiaojiang Liu, Jianhao Yan, Deng Cai, Huayang Li, and Jian Li. Learning to break the loop: Analyzing and mitigating repetitions for neural text generation, 2022. URL https://arxiv.org/abs/2206.02369.

Chiyuan Zhang, Samy Bengio, Moritz Hardt, Benjamin Recht, and Oriol Vinyals. Understanding deep learning requires rethinking generalization, 2017. URL https://arxiv.org/abs/1611.03530.

Chiyuan Zhang, Samy Bengio, Moritz Hardt, Benjamin Recht, and Oriol Vinyals. Understanding deep learning (still) requires rethinking generalization. Commun. ACM, 64(3):107–115, February 2021. ISSN 0001-0782. doi: 10.1145/3446776. URL https://doi.org/10.1145/3446776.

Peiyuan Zhang, Guangtao Zeng, Tianduo Wang, and Wei Lu. Tinyllama: An open-source small language model. CoRR, abs/2401.02385, 2024. URL https://arxiv.org/abs/2401.02385.

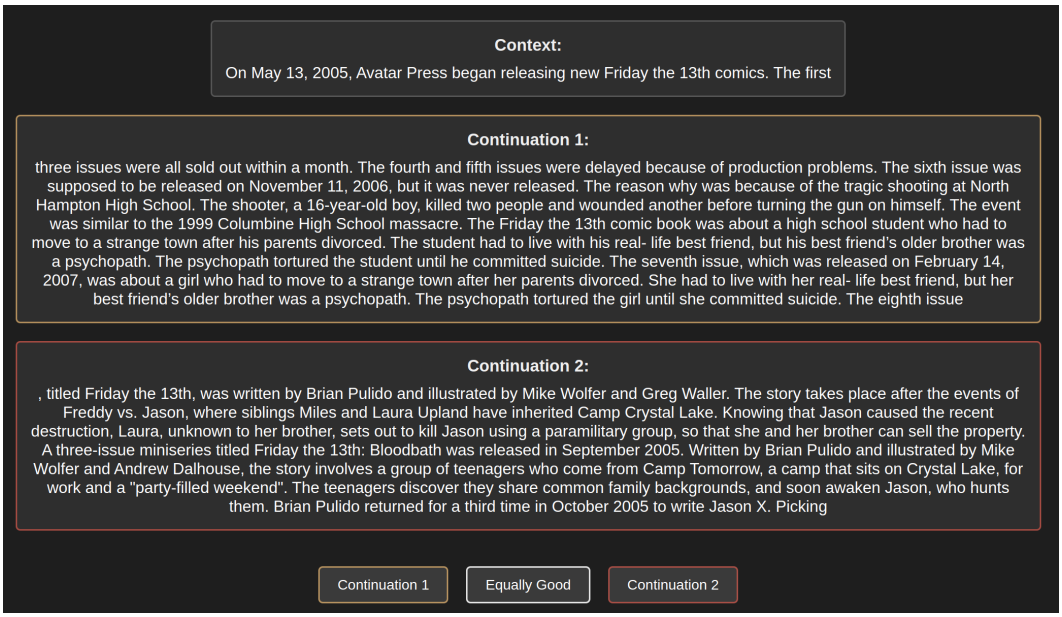

Figure 8: Screenshot of the interface used by the annotators. The example texts are from the 256 token scenario.

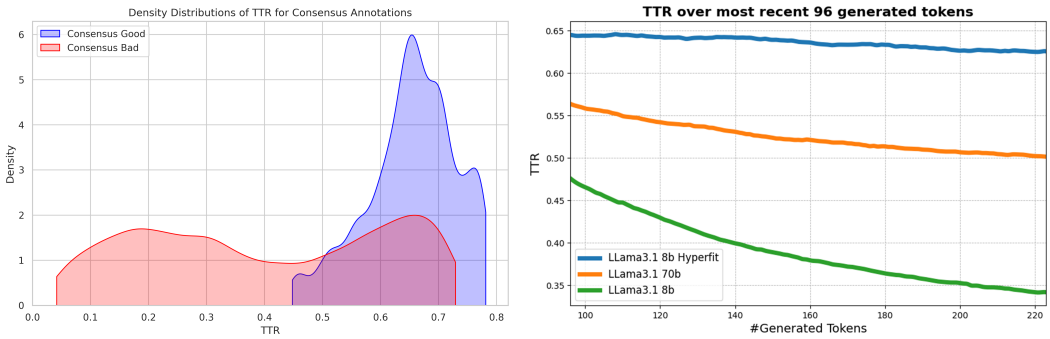

Figure 9: **Left**: TTR distributions of generated texts where all three annotators agreed on their quality, with 5% of outliers filtered away **Right**: TTR of the 96 most recent tokens in relation to the currently generated sequence length.

A Human Annotation

The research reported in this paper involved an extensive human evaluation for comparing text continuations resulting in a collection of over 20,000 annotations. In the interest of fairness as well as data quality, annotators were hired as freelancers and paid 10 USD per hour of annotation. All annotations were conducted through a simple web interface, where hired annotators could log in to their individual accounts. A screenshot of this interface is shown in Figure 8.

Using the annotation interface, annotators were continuously provided with a stream of randomly selected samples from the pool of those that had yet to receive three independent annotations. The order in which the model-generated text was displayed as either the first or second continuation was uniformly randomized.

A.1 TTR AS AN AUTOMATIC METRIC

The rudimentary metric of TTR measures the ratio of unique tokens in a sequence. Since this metric is highly affected by sequence length, we always apply it to the 96 lasts tokens of a generated sequence. Although TTR tells us nothing about the content of those tokens, in the context of longer texts generated by LLMs, we nevertheless find it to correlate human preferences. The left part of Figure–9 shows the TTR distribution of generated sequences (5% of outliers were filtered away for clarity) where the annotators were in consensus regarding their quality

The consensus distributions clearly show that texts with low TTR are less likely to be preferred. Indeed, below a certain threshold of about 0.4, no generated text reaches a good consensus. While there are samples with high TTR that are agreed upon to be bad, this suggests that a lower average TTR correlates with a higher probability of texts being of lower quality.

We note that the reason TTR is effective is that contemporary LLMs struggle with loops and repetitions over longer sequences. Indeed, due to the potential accumulation of errors during generation, the longer the generated sequence, the higher the chance of degenerative behavior and a lower TTR. This is clearly demonstrated in the right part of Figure 9, which shows the TTR of the 96 most recent tokens in relation to the currently generated sequence length, for the texts in Section 4. Although all models show some decrease in TTR as the sequence length increases, the hyperfitted Llama 3.1 both starts at a higher value and decreases at a slower rate than the original models.

B ADDITIONAL EXPERIMENTS

B.1 IMAGE GENERATION

In this section, we present additional details from our image generation experiments using ImageGPT-Large (774M parameters) on CIFAR-10. The model was hyperfitted on 2,000 randomly selected images for 50 epochs, using a learning rate of 3×10^{-3}. ImageGPT models converged more slowly, so we trained the models for 50 epochs with the effective batch size of 8, evaluating them at the end of each epoch on a validation set of 128 images. The changes in training and validation loss are shown in Figure 10.

To visually assess the effect of hyperfitting, we generated images using the first 256 pixels (8 rows) of entire CIFAR-10 test set, which were not seen during either pretraining or hyperfitting. Compared to the pre-trained model, the hyperfitted version produced sharper and more coherent images, with fewer repetitive patterns and greater structural consistency whilst producing diverse images. Figure 11 presents some examples of images generated by the original and hyperfitted models based on these prompts.

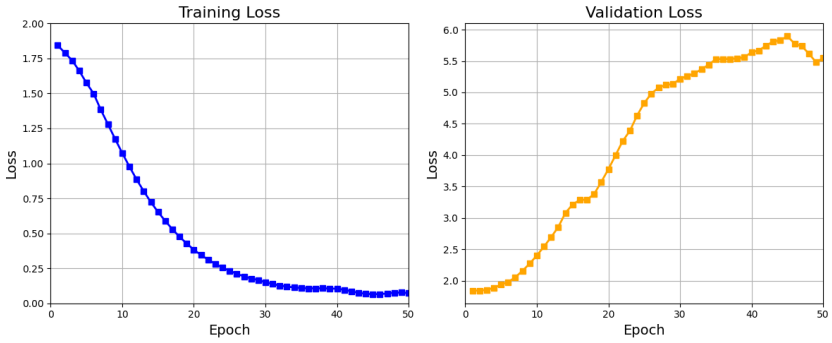

Figure 10: Training and validation loss curves for hyperfitted ImageGPT model.

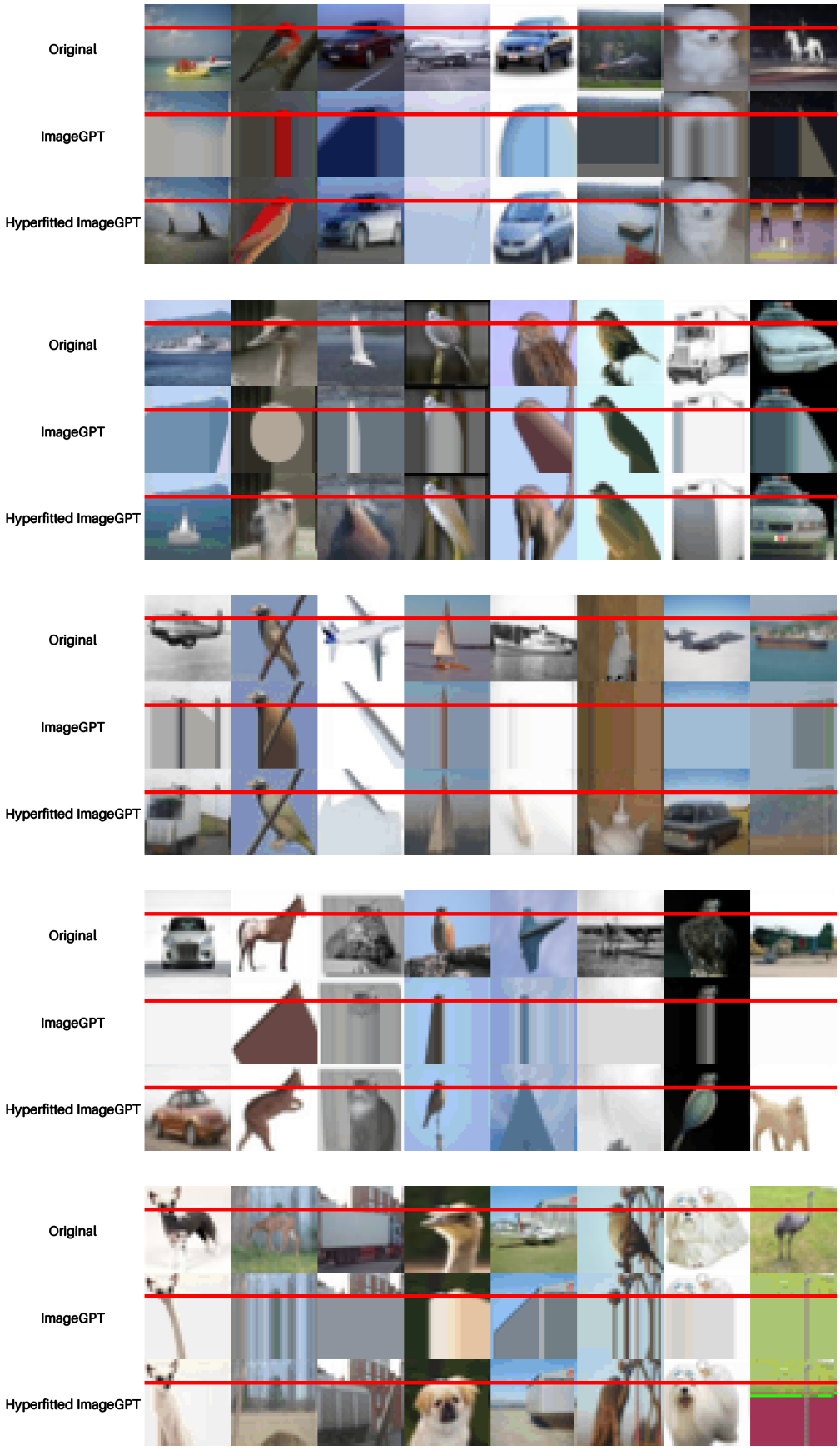

Figure 11: More examples of generated images using the original and hyperfitted ImageGPT (large).

Table 5: Ratio of 224-token generated sequences that contain an overlap of more than 5 tokens with the Fiction hyperfitting data.

Model	Fiction	Wikipedia	BBC News	Average
Original Models				
TinyLLama (1.1B)	29	11	14	18
DeepSeek (7B)	63	18	27	36
Llama 3.1 (8B)	38	4	8	16.7
Hyperfitted Models				
TinyLLama (1.1B)	89	45	47	60.3
DeepSeek (7B)	89	5	30	41.3
Llama 3.1 (8B)	85	4	29	39.3

B.2 Dataset-Specific Citation Blocking

As detailed in Section 3, the citation blocker works by pattern matching against the Fiction dataset. If the recent 5 tokens exists as a subsequence in the dataset, further generations on that subsequence is blocked, as soon as the current word has finished. Table 5 contains the ratio of generated sequences that exceeded the 5 token overlap at least once.

These results clearly show that all models, including the original ones, are more likely to generate sequences that overlap with the fiction data when generating from the fiction dataset. This is intuitive, as one would expect a higher overlap of phrases and expressions between different fiction texts, compared to Wikipedia and BBC News. However, it is evident that all hyperfitted models exhibit an increased ratio of overlaps when generating from fiction contexts. Notably, when generating from Wikipedia and BBC News, this increase is primarily observed with the TinyLlama model.

B.3 Instruction-tuned Models

Although this paper mainly focuses on models trained via next-token prediction, this section provides preliminary experiments on how hyperfitting affects already instruction-tuned models. Hence, we hyperfit the official instruct versions of DeepSeek 7B and LLama 3.1 with the same procedure and data as described in Section 3. We note that the full instruction-tuning procedure of these models is not disclosed.

Identically to how texts are generated in Section 4, we generate new texts for the 300 contexts using greedy decoding, meaning we simply generate the next token without any additional instruction prompt. For these generated sequences, we report the TTR of the tail-end 96 tokens, along with the model's perplexity on the original context. Additionally, we report the model's average predicted probability mass in the top-1 and top-3 tokens.

From the results in Table 6, it is clear that very similar trends emerge when applying hyperfitting to an instruction-tuned model. Perplexity increases, TTR remains more stable as sequence length increases, and the predicted distributions get narrower. Noticeably, however, the same trend appears to a smaller degree when comparing the original base models to the instruction-tuned models.

B.4 Performance on Downstream Tasks

We further explore the effect of hyperfitting on downstream tasks using the MMLU (Hendrycks et al., 2021) benchmark and GLUE benchmark (Wang et al., 2018). MMLU measuring the knowledge of the model,and GLUE being more task oriented. For both these tests we do not apply any further fine-tuning, and instead use the model's hyperfitted on the Fiction dataset as described in Section 3.

As instruction-tuned model's tend to perform significantly better in the MMLU benchmark, we include results for these models as well. As elaborated upon in Appendix B.3, these are trained via the same procedure as in that of Section 3.

B.4.1 MMLU

The MMLU dataset is a benchmark designed to measure a model's acquired knowledge over 57 subjects. This is achieved via a multiple-choice setup, where the candidate answer with the highest predicted probability is interpreted as the model's answer. Following the implementation of the official GitHub repository [5], we vary the number of question-answer pairs in the context and report these separately. Additionally, we calculate the models' perplexity on the zero-shot context of each question separately.

The results displayed in Table 7 show a clear trend where the hyperfitted models perform slightly worse overall. For DeepSeek, the drop in performance is roughly 1 accuracy point for both the base and instruct models. For the LLaMA 3.1 models, the drop is slightly bigger, with a 6-point decrease for the base model and a 5-point decrease for the instruct models.

The increase in perplexity for hyperfitted models is significantly smaller compared to the open-ended text generation experiment in Section 4. For example, the hyperfitted base version of LLaMA 3.1 increases from 8.7 to 12.3, whereas in Table 1, we see an increase from 36 to 389. A likely explanation for this is that the text of the MMLU questions leaves less room for subjective prediction, which is supported by the very low perplexity scores of all original models. As Section 5 demonstrates, hyperfitted models retain linguistic knowledge and will correctly assign probability when the next token is forced.

B.4.2 GLUE

The GLUE dataset tasks the model across a range of different tasks. For all these tasks we evaluate the models in both a few-shot and zero-shot setting. For the few-shot, we include the maximum number of shots allowed by the context length for each task, ranging from 1 to 4 shots. The shots were randomly selected from the training data while maintaining the label distribution of the original training set. The models were evaluated on the development sets as the test set labels are not publicly available.

Table 8 shows that hyperfitting has a very small impact on most tests, and no large overall trend emerges. Hence, similarly to the results in Appendix B.4.1, we conclude that the overall downstream capabilities of the models remain mostly intact, and hyperfitting does not lead to catastrophic degradation in performance across tasks.

[5] https://github.com/hendrycks/test

Table 6: Distributions predicted for the original texts (context + continuation) in Section 4. @N indicating the accumulated probability of the N:th tokens with the highest probability.

Model	Context PPL	128 TTR	256 TTR	@1 Prob	@3 Prob
Original Models					
DeepSeek (7B)	34	45.6	32.2	49.1	67.3
Llama 3.1 (8B)	29	56.4	50.6	48.4	67.1
DeepSeek (7B) Chat	49	57.6	56.2	53.0	71.5
Llama 3.1 (8B) Chat	45	58.9	55.7	50.1	69.6
Hyperfitted Models					
DeepSeek (7B)	545	62.3	60.5	74.5	90.0
Llama 3.1 (8B)	389	64.5	62.6	74.4	89.2
DeepSeek (7B) Chat	547	63.3	63.3	75.0	90.2
Llama 3.1 (8B) Chat	384	63.6	62.0	74.0	89.3

Table 7: Results on MMLU dataset for different number of question-answer pairs included in the prompt. The perplexity score is measured on the zero-shot context of all questions.

Model	**Perplexity**	**0-Shot**	**1-Shot**	**3-Shot**	**5-Shot**
Original Models					
DeepSeek (7 B)	9.3	46.4	47.3	48.8	49.4
Llama 3.1 (8 B)	8.7	65.4	66.0	66.5	66.6
DeepSeek (7 B) Chat	11.4	51.5	50.3	51.7	51.8
Llama 3.1 (8 B) Chat	10.9	68.5	68.2	68.6	68.9
Hyperfitted Models					
DeepSeek (7 B)	32.3	44.5	46.6	48.1	48.4
Llama 3.1 (8 B)	12.1	58.9	59.9	59.7	60.2
DeepSeek (7 B) Chat	32.3	49.7	50.3	50.6	50.9
Llama 3.1 (8 B) Chat	16.7	63.1	63.0	63.6	64.4

Table 8: Comparison of the original and hyperfitted Llama and Deepseek models across various GLUE tasks, using 0-shot (0S) and few-shot (FS) configurations. The target metrics are accuracy (acc), F1 score (f1), and Matthews correlation (corr.).

		DeepSeek (7B)				LLama 3.1 (8B)			
		Base		Hyperfitted		Base		Hyperfitted	
Task	Metric	0S	FS	0S	FS	0S	FS	0S	FS
cola	corr.	0.	0.362	0.	0.268	0.215	0.538	0.240	0.297
mnli	acc	0.179	0.352	0.088	0.352	0.	0.649	0.004	0.570
mrpc	acc	0.	0.684	0.478	0.691	0.679	0.684	0.642	0.703
	f1	0.	0.812	0.573	0.816	0.786	0.812	0.775	0.797
qnli	acc	0.464	0.573	0.497	0.626	0.710	0.579	0.420	0.548
qqp	acc	0.055	0.680	0.398	0.649	0.589	0.806	0.271	0.756
	f1	0.042	0.279	0.239	0.102	0.619	0.732	0.418	0.667
rte	acc	0.	0.430	0.354	0.574	0.	0.599	0.646	0.690
sst2	acc	0.594	0.943	0.718	0.923	0.847	0.898	0.393	0.904

C TEXT GENERATION EXAMPLES

C.1 HYPERFITTING AND ORIGINAL MODELS

Context - Fiction:

He thought of his family and their recent vacation to Jamaica and all the fun they had. He smiled as he remembered his wife screaming

TinyLlama 1.1B - Original

when he told her he was going to be a dad. He had to tell her he was going to be a dad. He had to tell her he was going to be a dad. He had to tell her he was going to be a dad. He had to tell her he was going to be a dad. He had to tell her he was going to be a dad. He had to tell her he was going to be a dad. He had to tell her he was going to be a dad. He had to tell her he was going to be a dad. He had to tell her he was going to be a dad. He had to tell her he was going to be a dad. He had to tell her he was going to be a dad. He had to tell her he was going to be a dad. He had to tell her he was going to be a dad. He

TinyLlama 1.1B - Hyperfitted

in joy after she saw the ring on his finger. She had been a treasured wife, and he was treasured husband. He loved the way it felt to be loved unconditionally. He loved that no matter what she would be his number one fan. No matter what the occasion he would be the life of the party! He would be the happiest man alive! CHAPTER 2 THE DAY OF THE WEDDING The bride and her mother arrived in the great hall. The hall was where all the wedding guests were gathered. The hall was also where the wedding dinner was served. "Are you sure this hall can hold all of our guests?" The bride asked as she looked at the large hall. "Yes I am." The groom replied. "Then I think that we should have dinner here this evening." The bride said. "Oh no! I haven't tasted food in a long time!" Mother exclaimed as she followed the bride into the large hall. "Let me show you where the kitchen is." The bride said to her

Context - BBC News:
Negative press coverage of Manchester City forward Raheem Sterling "emboldens racist rhetoric", says the Professional Footballers' Association.

DeepSeek 7B - Original

The PFA said it was "deeply concerned" by the "unacceptable" comments made by former England striker Stan Collymore. Collymore said Sterling should "go back to Africa" and "stop being a disgrace". The PFA said it was "disappointed" that the comments were not condemned by the Football Association. Sterling, 20, has been the subject of racist abuse on social media since he was substituted during England's 2-0 defeat by Germany in the World Cup semi-final. The PFA said it was "disappointed" that the FA had not condemned Collymore's comments. "The PFA is deeply concerned by the comments made by Stan Collymore," said the union. "The PFA is disappointed that the FA has not condemned these comments and we hope that the FA will take the appropriate action to ensure that this type of behaviour is not tolerated." The PFA said it was "disappointed" that the FA had not condemned Collymore's comments The PFA said it was "disappointed"

DeepSeek 7B - Hyperfitted

The 20-year-old has been the subject of abuse on social media after he was involved in a training ground bust-up with Liverpool defender Joe Gomez. PFA chief executive Gordon Taylor told BBC Radio 5 live: "What we've seen in the last 48 hours is a complete lack of respect for a young man who is a fantastic footballer and a role model in his community. "What we've also seen is a complete lack of respect for the PFA, the players' union, and what we stand for. "We will not be lectured by anyone about what we should and shouldn't do. "We are a union that represents all players, past and present, and we will not be told what to do by anyone." The PFA has more than 11,000 members, including all current Premier League players as well as many from the lower leagues and abroad. Mr Taylor said the organisation would be "monitoring" the situation and would take "whatever action is necessary" to support Mr Sterling. He added: "We will not be lectured by anyone about

Context - Wikipedia:
After the Louisiana Purchase, Breckinridge focused on securing a vote to present the Twelfth Amendment to the states for ratification.

Llama 3.1 8B - Original

The amendment was designed to prevent a repeat of the 1800 election, in which the House of Representatives had to choose between the two candidates with the most electoral votes. The Twelfth Amendment, which was ratified in 1804, required electors to vote separately for president and vice president. Breckinridge also worked to secure the passage of the Judiciary Act of 1801, which created new federal courts and expanded the jurisdiction of the Supreme Court. The act was designed to strengthen the federal judiciary and to ensure that the federal government had the power to enforce its laws. Breckinridge was a strong supporter of the War of 1812 and served as a colonel in the Kentucky militia during the conflict. He was also a member of the Kentucky legislature and served as a delegate to the Hartford Convention in 1814. After the war, Breckinridge returned to Kentucky and served as a member of the state legislature and as a judge on the Kentucky Court of Appeals. He was also a member of the Kentucky Constitutional Convention in 1834. Breckinridge was a strong supporter of the Whig Party and

Llama 3.1 8B - Hyperfitted

The amendment had been defeated in the Senate in 1804, and there was little chance of it passing if presented to the states in its current form. Breckinridge, working with Senate Judiciary Committee chairman William Pinkney (D-MD) and Virginia senator George Hay (D-VA), crafted a compromise version of the amendment that was acceptable to both parties. In the spring of 1805, the Senate voted 32 to 22 to submit the amendment to the states for ratification. By October 1805, eleven of the twelve state legislatures had approved the amendment, and in December 1805, the remaining state, Delaware, ratified the measure. The Twelfth Amendment, which modified the Electoral College system, was thus added to the Constitution. The amendment was intended to correct what had become known as the "three-fifths rule", by which the number of electoral votes cast by a state was equal to the number of senators plus the number of representatives in Congress. This gave small states, which had fewer representatives than larger states, an electoral advantage. The amendment changed the method of awarding electoral votes

C.2 DIFFERENT HYPERFITTING DATASETS

Context:
"This vaccine is more than good news, it's a game changer," Dr Mohammed Khaki tells Newsbeat.

LLama 3.1 - Hyperfitted Fiction

The vaccine, which was developed by Oxford University, is currently being trialled in several countries, including the UK, China, and the US. It has shown promising results in early tests, and if successful, could be rolled out to the public as early as next year. "What makes this vaccine so effective is that it targets multiple strains of the virus," Dr Khaki explains. "This means that it can protect against a wider range of variants, which is especially important as the virus continues to evolve." The doctor says that while the vaccine is not a cure for COVID-19, it will significantly reduce the severity of the disease. This, he says, will be especially helpful for vulnerable groups, such as the elderly and those with underlying health conditions. "We know that COVID-19 can be a deadly disease, but we also know that there are things we can do to protect ourselves," Dr Khaki says. "Washing your hands regularly, wearing a mask, and avoiding close contact with those who are sick are all important steps you can take to stay safe." However, he acknowledges that the pandemic is far from over, and

LLama 3.1 - Hyperfitted News

"It will not only protect us from the current pandemic but will also prevent future pandemics by protecting us from getting infected in the first place." The technology is based on a natural protein found in the lining of the nose called angiotensin-converting enzyme 2 (ACE2). Coronavirus uses this protein to enter the body so the vaccine has been designed to target it. "The vaccine will train our bodies to produce antibodies that will coat the surface of the nose and prevent the virus from entering the body," Dr Khaki explains. "It will also train our bodies to produce memory cells that will remain in our system and provide long-term protection against future infections." The doctor says the best way to think of the vaccine is not as a magic bullet but as a way to "train our bodies to fight the virus in the most efficient way". "The virus will continue to change and adapt and our bodies will need to continue to change and adapt in order to stay one step ahead of the virus," he says. "There is no such thing as a perfect vaccine but the goal is to make the best possible vaccine that we can." There are two vaccines currently being administered to

LLama 3.1 - Hyperfitted Wikipedia

"Having a vaccine that is effective against all human papillomavirus types should increase uptake and help to protect against the most common sexually transmitted infection in the UK. "HPV infection can cause significant health problems, including genital warts and cancer, and while the vaccine is not a cure for these conditions, it should help to prevent them occurring in the first place." Dr Khaki says that while the vaccine has been shown to be effective in trials, it will only be licensed for use once the manufacturing process has been completed and the vaccine has been given to thousands of people in the real world. "Once we have that data, we will be able to say with more certainty how effective the vaccine is and what its side effects are," he says. "Until then, we have to be a little bit cautious, although from what we know already, it looks very promising." The vaccine is expected to be given to 12 to 13-year-olds, in line with the HPV immunisation programme that is already underway in Scotland. It is also likely to be given to young women and men who have not already been immunised, in order to provide them